Intracellular Metabolic Fate of Radioactivity after Injection of Technetium-99m-Labeled Hydrazino Nicotinamide Derivatized Proteins

ARTICLE *in* BIOCONJUGATE CHEMISTRY · MAY 1999

Impact Factor: 4.51 · DOI: 10.1021/bc980105f · Source: PubMed

9 AUTHORS, INCLUDING:

Yasushi Arano
Chiba University
217 PUBLICATIONS **2,052** CITATIONS
SEE PROFILE

Kazuma Ogawa
Kanazawa University
67 PUBLICATIONS **909** CITATIONS
SEE PROFILE

Intracellular Metabolic Fate of Radioactivity after Injection of Technetium-99m-Labeled Hydrazino Nicotinamide Derivatized Proteins

Masahiro Ono,[†] Yasushi Arano,*[,†] Tomoya Uehara,[†] Yasushi Fujioka,[†] Kazuma Ogawa,[†] Shinji Namba,[†] Takahiro Mukai,[‡] Morio Nakayama,[§] and Hideo Saji[†]

Department of Patho-Functional Bioanalysis, Graduate School of Pharmaceutical Sciences, Kyoto University, Yoshida-shimoadachi-cho, Sakyo-ku, Kyoto 606-8501, School of Pharmaceutical Sciences, Nagasaki University, 1-14 Bunkyo-machi, Nagasaki 852-8131, Department of Radiopharmaceutical Chemistry, Faculty of Pharmaceutical Sciences, Kumamoto University, Oe-Honmachi, Kumamoto 862-0973, Japan.
Received September 9, 1998; Revised Manuscript Received February 8, 1999

Hydrazino nicotinate (HYNIC) has been shown to produce technetium-99m (^{99m}Tc)-labeled proteins and peptides of high stability with high specific activities. However, persistent localization of radioactivity was observed in nontarget tissues such as the liver and kidney after administration of [^{99m}Tc]HYNIC-labeled proteins and peptides, which compromises the diagnostic accuracy of the radiopharmaceuticals. Since lysosomes are the principal sites of intracellular catabolism of proteins and peptides, ^{99m}Tc−HYNIC-labeled galactosyl-neoglycoalbumin (NGA) was prepared using tricine as a co-ligand to investigate the fate of the radiolabel after lysosomal proteolysis in hepatocytes. When injected into mice, over 90% of the injected radioactivity was accumulated in the liver after 10 min injection. At 24 h postinjection, ca. 40% of the injected radioactivity still remained in liver lysosomes. Size-exclusion HPLC analyses of liver homogenates at 24 h postinjection showed a broad radioactivity peak ranging from molecular masses of 0.5−50 kDa. RP-HPLC analyses of liver homogenates suggested the presence of multiple radiolabeled species. However, most of the radioactivity migrated to lower molecular weight fractions on size-exclusion HPLC after treatment of the liver homogenates with sodium triphenylphosphine-3-monosulfonate (TPPMS). The TPPMS-treated liver homogenates showed a major peak at a retention time similar to that of [[^{99m}Tc](HYNIC−lysine)(tricine)(TPPMS)] on RP-HPLC. Similar results were obtained with urine and fecal samples. These findings suggested that the chemical bonding between ^{99m}Tc and HYNIC remains stable in the lysosomes and following excretion from the body. The persistent localization of radioactivity in the liver could be attributed to the slow elimination rate of the final radiometabolite, [[^{99m}Tc](HYNIC−lysine)(tricine)$_2$], from lysosomes, and subsequent dissociation of one of the tricine co-ligands in the low pH environment of the lysosomes in the absence of excess co-ligands, followed by binding proteins present in the organelles. The findings in this study also suggested that the development of appropriate co-ligands capable of preserving stable bonding with the Tc center is essential to reduce the residence time of radioactivity in nontarget tissues after administration of [^{99m}Tc]HYNIC-labeled proteins and peptides.

INTRODUCTION

Radiopharmaceuticals derived from low molecular weight peptides and antibody fragments have been used for visualization of the sites of tumors, infections, and thromboses at early postinjection times (*1*−*3*). The pharmacokinetics of these molecules are well matched with the physical half-life of ^{99m}Tc, the most widely used and the least expensive radionuclide for external imaging. Some peptides contain the N_4 tetraamide (Gly-Gly-Gly), N_3S triamidethiol (Gly-Gly-Cys), or N_2S_2 diamidedithiol (Cys-Gly-Cys) tripeptide sequence (*4*−*7*), which form stable ^{99m}Tc complexes with the $[Tc{=}O]^{3+}$ core. However, the radiolabeling of these tripeptide sequences may require harsh conditions such as high pH and high temperatures. In addition, ^{99m}Tc labeling may lead to the loss of receptor-binding affinity if the tripeptide sequence constitutes part of the receptor-binding motif. Furthermore, some peptides and proteins do not possess such endogenous binding sites to form ^{99m}Tc chelate with high stability. Thus, attachment of appropriate chelating agents to proteins or peptides constitutes a major strategy for labeling of these molecules with ^{99m}Tc for in vivo applications.

Hydrazino nicotinate (HYNIC) is one of the most attractive bifunctional coupling agents for labeling of peptides and proteins with ^{99m}Tc. Indeed, HYNIC provides ^{99m}Tc-labeled nonspecific human IgG, human serum albumin, Fab fragment, chemotactic peptides, and RGD peptides with high specific radioactivities and high radiochemical yields (*8*−*13*). Previous studies indicated that HYNIC acts as a monodentate or bidentate ligand to form a mixed ligand ^{99m}Tc complex in the presence of appropriate co-ligands such as glucoheptonate or tricine (*8*, *14*). Both Tc−hydrazido and Tc−diazenido bonds have been reported and characterized by X-ray crystallography (*15*−*19*). A recent study also suggested that HYNIC

* To whom correspondence should be addressed. Phone: 81-75-753-4608. Fax: 81-75-753-4568. E-mail: arano@pharm.kyoto-u.ac.jp.
[†] Graduate School of Pharmaceutical Sciences, Kyoto University.
[‡] School of Pharmaceutical Sciences, Nagasaki University.
[§] Faculty of Pharmaceutical Sciences, Kumamoto University.

10.1021/bc980105f CCC: $18.00
Published on Web 04/29/1999

requires two tricine ligands to complete the coordination sphere regardless of whichever type of bond ^{99m}Tc and HYNIC may form (*12*).

When administered in vivo, [^{99m}Tc]HYNIC-labeled proteins and peptides show localization of radioactivity in target tissues. However, high and persistent radioactivity levels were also observed in the liver and kidney where catabolism of the parent proteins and peptides occurs, which compromises the diagnostic accuracy of these radiopharmaceuticals (*8*, *20*−*22*). Since indium-111 (^{111}In)-labeled proteins and peptides also show persistent localization of radioactivity in tissues in which they are catabolized due to the slow elimination rates of the final radiometabolites generated after lysosomal proteolysis in these tissues (*23*−*27*), similar mechanisms may be responsible for the long residence times of the radioactivity derived from [^{99m}Tc]HYNIC-labeled proteins and peptides in these tissues. Decomposition or exchange reactions of the [^{99m}Tc]HYNIC−tricine mixed ligand complex may also account for the long residence times of the radioactivity in the lysosomal compartment where the complexes are present at very low ligand concentrations in the low pH environment. Indeed, decomposition of a [^{99m}Tc]HYNIC-conjugated peptide was indicated in a dilute solution (*12*). However, little is known regarding the retention of radioactivity at the sites of catabolism after administration of [^{99m}Tc]HYNIC-labeled proteins and peptides (*22*). Since HYNIC allows preparation of a variety of ^{99m}Tc-labeled proteins and peptides, the chemical design of HYNIC-based chelating agents that circumvent such undesirable localization of radioactivity is required. Thus, understanding of the fate of ^{99m}Tc after metabolism of [^{99m}Tc]HYNIC-labeled proteins and peptides is essential.

Since lysosomes are the principal sites of intracellular catabolism of proteins and peptides (*28*), metabolic analysis of [^{99m}Tc]HYNIC-labeled proteins in the lysosomal compartment of the liver or kidney would provide insight into the mechanisms responsible for the prolonged radioactivity levels in these organs. Galactosyl-neoglycoalbumin (NGA) is incorporated by hepatic parenchymal cells via receptor-mediated endocytosis immediately after administration (*29*). Use of NGA as a carrier protein provides explicit information regarding the fate of radioactivity after lysosomal proteolysis in hepatocytes without being affected by transchelation of radiolabels in plasma or redistribution of radiometabolites generated elsewhere in the body to the liver (*24*, *30*). In addition, a recent study indicated that an [^{111}In]DTPA-adduct of lysine was generated as the final radiometabolite in the liver and kidney when ^{111}In-labeled NGA and antibodies using cyclic DTPA dianhydride (cDTPA) as the bifunctional chelating agent (BCA) were administered into animals (*31*).

In the present study, NGA was used as a model protein, and biodistribution and subcellular localization of the radioactivity in the murine liver was investigated after administration of [^{99m}Tc]HYNIC-labeled NGA using tricine as the co-ligand. Radiometabolites retained in the liver and excreted from the body were analyzed to determine the fate of the radiolabel, ^{99m}Tc, after lysosomal proteolysis in hepatocytes. Factors affecting the long residence time of radioactivity in nontarget tissues after administration of [^{99m}Tc]HYNIC-labeled proteins and peptides will be discussed. Since HYNIC generates ^{99m}Tc-labeled proteins and peptides in the presence of two tricine co-ligands (*12*, *14*, *32*), ^{99m}Tc-labeled HYNIC−NGA and HYNIC−lysine are abbreviated as [[^{99m}Tc](HYNIC−NGA)(tricine)$_2$] and [[^{99m}Tc](HYNIC−lysine)(tricine)$_2$], respectively.

MATERIALS AND METHODS

Reagents and Chemicals. [^{99m}Tc]Pertechnetate ($^{99m}TcO_4^-$) was eluted in saline solution on a daily basis from Daiichi Radioisotope Laboratory generators (Chiba, Japan). Reversed-phase high-performance liquid chromatography (RP-HPLC) was performed with a Cosmosil 5 C_{18}-MS column (4.6 × 150 mm, Nacalai Tesque, Kyoto) at a flow rate of 1 mL/min with a gradient mobile phase starting from 100% A (0.1% aqueous trifluoroacetic acid) to 100% B (acetonitrile with 0.1% trifluoroacetic acid) in 30 min (solvent system 1). RP-HPLC was also performed with a gradient mobile phase starting from 10% acetonitrile in 0.05 M phosphate buffer (pH 7.0) to 90% acetonitrile in the same buffer in 20 min and the final solvent composition was maintained for a further 10 min (solvent system 2). Size-exclusion HPLC was performed using a 5 Diol-300 column (7.5 × 600 mm, Nacalai Tesque) connected to a 5 Diol-300 guard column (7.5 × 50 mm, Nacalai Tesque), eluted with 0.1 M phosphate buffer (pH 6.8) at a flow rate of 1 mL/min. The eluent was collected with a fraction collector (RediFrac; Pharmacia Biotech, Tokyo) at 30 s intervals, and the radioactivity levels in each fraction (500 μL) were determined with an auto well counter (ARC-2000; Aloka, Tokyo). TLC analyses were performed with silica plates (Merck Art 5553) with a mixture of 10% aqueous ammonium chloride-methanol (1:1) or saline as developing solvents. Proton nuclear magnetic resonance (^{1}H NMR) spectra were recorded on a Bruker AC-200 spectrometer, and the chemical shifts are reported in parts per million downfield from an internal tetramethylsilane standard. Fast atom bombardment mass spectra (FAB-MS) were obtained with a JMS-HX/HX 110 A model (JEOL Ltd., Tokyo). Sodium triphenylphosphine-3-monosulfonate (TPPMS) was purchased from Tokyo Kasei Kogyo Co. Ltd. (Tokyo), and other reagents were of reagent grade and used as received. To facilitate collection of urine and feces after administration of radiolabeled NGA, mice were housed in metabolic cages (Metabolica, MM type; Sugiyama-Gen Iriki Co. Ltd., Tokyo). Succinimidyl 6-hydrazinopyridine-3-carboxylate hydrochloride (SHNH) was synthesized according to the procedure of Abrams et al. (*8*).

Synthesis of Galactosyl-Neoglycoalbumin (NGA). Cyanomethyl-2,3,4,6-tetra-*O*-acetyl-1-β-galactopyranoside, synthesized according to the procedure of Lee et al. (*33*), was conjugated with human serum albumin (HSA, A-3782; Sigma Co., St. Louis, MO), according to the procedure of Stowell et al. (*34*). The phenol-sulfuric acid reaction (*35*) indicated that 43 galactose units were attached to each HSA molecule.

Synthesis of HYNIC−Lysine. Boc-protected SHNH (500 mg, 1.43 mmol), prepared by the method of Abrams et al. (*8*), in 15 mL of dry acetonitrile was added to a solution of α-Boc-L-lysine (352 mg, 1.43 mmol) in saturated $NaHCO_3$ (5 mL) at 0 °C. The reaction mixture was stirred at room temperature for 6 h. After filtration to remove white precipitates, the filtrate was cooled to 0 °C, and the solution was acidified to pH 2−3 with concentrated H_2SO_4 before extraction with ethyl acetate (20 mL × 4). The organic layers were combined and dried over anhydrous calcium sulfate. After removing the solvent in vacuo, the oily residue was chromatographed on silica gel using a mixture of chloroform-methanol-acetic acid (10:1:0.1) as the eluent to produce Boc-HYNIC-

α-Boc-L-lysine as white crystals (532 mg, 75.9%). ^{1}H NMR (CD_3OD): δ 1.26−1.81 [6H, m, $(CH_2)_3$], 1.43 (9H, s, Boc), 1.46 (9H, s, Boc), 3.39 (2H, t, NCH_2), 4.23 (1H, q, CH), 6.46 (1H, d, pyridine), 7.82 (1H, dd, pyridine), 8.10 (1H, d, pyridine). Anal. calcd for $C_{22}H_{35}O_7N_5 \cdot CH_3COOH$: C, 53.23; H, 7.21; N, 12.94. Found: C, 53.06; H, 7.04; N, 12.88. FAB-MS calcd for $C_{22}H_{36}O_7N_5$ (MH^+): *m/z* 482. Found: *m/z* 482.

Boc-HYNIC-α-Boc-L-lysine dissolved in 2 mL of dry ethyl acetate was added to a solution of 4 N HCl prepared in 2 mL of dry ethyl acetate. The reaction mixture was stirred at room temperature for 1 h. The HCl salt of HYNIC−lysine precipitated as white crystals (160 mg, 91.4%). ^{1}H NMR (DMSO-d_6): δ 1.36−1.87 [6H, m, $(CH_2)_3$], 3.24 (2H, t, NCH_2), 3.86 (1H, q, CH), 6.93 (1H, d, pyridine), 8.16 (1H, dd, pyridine), 8.67 (1H, d, pyridine). Anal. calcd for $C_{12}H_{21}O_3N_5Cl_2 \cdot 1/3\ C_4H_{10}O \cdot 3H_2O$: C, 37.66; H, 6.60; N, 16.47. Found: C, 37.65; H, 6.88; N, 16.35. FAB-MS calcd for $C_{12}H_{20}O_3N_5$ (MH^+): *m/z* 282. Found: *m/z* 282.

Preparation of HYNIC−NGA Conjugate. The conjugation reaction of HYNIC with NGA was performed according to the procedure of Abrams et al. (*8*) with slight modifications as follows: Briefly, 10 μL of SHNH (8.3 mg/100 μL) in dimethyl sulfoxide (DMSO) was added dropwise to a 1 mL of stirred NGA solution (20 mg/mL) in 0.15 M borate buffer (pH 8.5). The solution was stirred gently for 2 h at room temperature protected from the light. The HYNIC−NGA conjugate was purified by Sephadex G-50 (Pharmacia Biotech Co. Ltd., Tokyo) column chromatography (1.8 × 40 cm) equilibrated and eluted with 10 mM citrate buffer (pH 5.2). The protein fractions were subsequently concentrated to 5 mg/mL by ultrafiltration (8 MC model, Amicon Grace, Tokyo). The number of HYNIC groups attached per molecule of NGA was determined by measuring the hydrazino groups with *p*-nitrobenzaldehyde, according to the method of King et al. (*36*).

^{99m}Tc Labeling of HYNIC−NGA and HYNIC−Lysine. To a solution of HYNIC−NGA (100 μL; 5.0 mg/mL) in 10 mM citrate buffer (pH 5.2) was added an equal volume of [^{99m}Tc]tricine$_2$ prepared by the method of Larsen et al. (*14*), and the mixture was incubated for 1 h at room temperature. [[^{99m}Tc](HYNIC−NGA)(tricine)$_2$] was purified by the centrifuged column procedure using a Sephadex G-50 column equilibrated and eluted with 0.1 M phosphate buffer (pH 7.0) (*37*). Radiochemical yields of [[^{99m}Tc](HYNIC−NGA)(tricine)$_2$] were determined by size-exclusion HPLC and TLC developed with saline. In a control study, unmodified NGA was labeled with [^{99m}Tc]tricine$_2$, according to the procedures described above.

A solution of [^{99m}Tc]tricine$_2$ (100 μL) was added to a 100 μL of HYNIC−lysine solution (2 mg/mL) in 10 mM citrate buffer (pH 5.2), and the reaction mixture was incubated for 1 h at 37 °C. Radiochemical yields were assessed by size-exclusion HPLC, RP-HPLC, and TLC developed with a mixture of 10% aqueous ammonium chloride-methanol (1:1).

[[^{99m}Tc](HYNIC−Lysine)(Tricine)(TPPMS)] Ternary Mixed Ligand Complex. A solution of [[^{99m}Tc](HYNIC−lysine)(tricine)$_2$] (100 μL) prepared as described above was mixed with 100 μL of TPPMS solution (5 mg/mL) in 0.1 M acetate buffer (pH 3.0). The solution was acidified to pH 3 with 0.1 N HCl and incubated at 37 °C for 1 h. The reaction mixture was analyzed by RP-HPLC, size-exclusion HPLC and TLC developed with a mixture of 10% aqueous ammonium chloride-methanol (1:1).

Plasma Stability of [[^{99m}Tc](HYNIC−NGA)(Tricine)$_2$]. [[^{99m}Tc](HYNIC−NGA)(tricine)$_2$] was diluted 20-fold with freshly prepared murine plasma, and the solution was incubated at 37 °C for 24 h. After 1 and 24 h of incubation, 50 μL aliquots of the samples were drawn, and the radioactivity was analyzed by size-exclusion HPLC and TLC developed with saline.

In Vivo Studies. The protein concentration of [[^{99m}Tc](HYNIC−NGA)(tricine)$_2$] was adjusted to 90 μg/mL with saline. Biodistribution studies were performed by the intravenous administration of [[^{99m}Tc](HYNIC−NGA)(tricine)$_2$] to 6-week-old male ddY mice (27−30 g) (*38*). Groups of five mice each were administered 9 μg (37−56 KBq) of [[^{99m}Tc](HYNIC−NGA)(tricine)$_2$] prior to sacrificing the animals at 10 and 30 min and 1, 3, 6, and 24 h postinjection by decapitation. Previous studies indicated that under these conditions radiolabeled NGAs are incorporated by parenchymal cells of murine liver via receptor-mediated endocytosis (*24*, *30*). Tissues of interest were removed, weighed and the radioactivity counts were determined with an auto well γ counter (ARC 2000). To determine the amounts and routes of excretion of radioactivity from the body, mice were housed in metabolic cages for 24 h after administration of [[^{99m}Tc](HYNIC−NGA)(tricine)$_2$], and urine and feces were collected and the radioactivity was determined.

The subcellular distribution of radioactivity in the murine liver was investigated by perfusing the organ in situ with cold 0.25 M sucrose buffered with 10 mM phosphate buffer (pH 7.4) at 1 and 24 h postinjection of [[^{99m}Tc](HYNIC−NGA)(tricine)$_2$]. The liver was treated according to the procedure described previously (*24*, *30*). Briefly, the isolated organ was minced with scissors, suspended in 4 vol of the same buffer prior to homogenization by hand with a Dounce homogenizer (20 strokes). This was followed by two final strokes in an ice-cooled Potter-Elvehjem homogenizer with a Teflon pestle rotated at 800 rpm. The resulting homogenate was centrifuged twice for 5 min at 340 *g* at 4 °C. The isolated supernatant was then layered on top of iso-osmic (0.25 M sucrose) 37.5% Percoll (9 mL, Pharmacia Biotech Co. Ltd.) at a density of 1.08 g/mL. After centrifugation at 20000*g* (RP 30 rotor; Hitachi Co. Ltd., Tokyo) for 90 min at 4 °C, the gradients were collected in 14 fractions. β-Galactosidase was used as a marker enzyme for lysosomes (*39*, *40*) and its activity in each fraction was determined using *p*-nitrophenyl β-galactopyranoside as the substrate (*41*). The density and radioactivity counts of the respective fraction were also determined.

The radiolabeled species remaining in the liver at 1 and 24 h postinjection and excreted in the urine and feces by 24 h postinjection of [[^{99m}Tc](HYNIC−NGA)(tricine)$_2$] (133−266 KBq) were analyzed according to the procedure described previously (*24*, *30*). Briefly, the murine liver was perfused in situ with cold 0.1 M Tris-citrate buffer (pH 6.5) containing 0.15 M NaCl, 0.02% sodium azide, 1 TIU/mL aprotinin, 2 mM benzamidine-HCl, 2 mM iodoacetamide, 1 mM phenylmethanesulfonyl fluoride, and 5 mM diisopropyl fluorophosphate before the hepatic samples (1 g each) were isolated. Each tissue sample was placed in a test tube and subjected to three cycles of freezing (dry ice-acetone bath) and thawing. After addition of 5 vol of the same buffer containing an additional 35 mM β-octyl-glucoside, the samples were homogenized with a Polytron homogenizer (PT 10-35, Kinematica GmbH, Littau, Switzerland) set at full speed with three consecutive 30 s bursts prior to centrifugation at 48000*g* for 20 min at 4 °C (Himac CS-120 Centrifuge; Hitachi

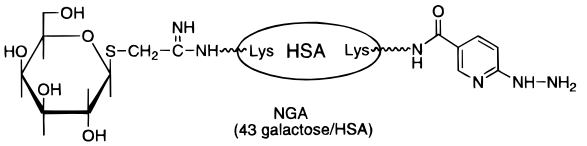

Figure 1. Chemical structure of HYNIC−NGA.

Co. Ltd., Tokyo). The supernatant was separated from the pellet, and the radioactivity was counted. In a procedure similar to that used for liver tissue, fecal samples were homogenized in the presence of 0.1 M phosphate buffer (pH 6.0) before centrifugation at 10000*g* for 20 min at 4 °C. The liver, feces, and urine samples were analyzed immediately by size-exclusion HPLC and TLC after filtration through a polycarbonate membrane with a pore diameter of 0.45 μm (Nacalai Tesque). Each sample was also analyzed immediately by RP-HPLC after ultrafiltration with a 10 kDa cutoff membrane (Microcon-10, Amicon).

Since TPPMS forms a ternary mixed ligand complex with [[^{99m}Tc](HYNIC−peptide)(tricine)$_2$] (*32*), the liver homogenates were reacted with TPPMS and the reaction products were analyzed to further characterize the radiometabolites retained in the liver. The supernatants of the liver homogenates (100 μL) were mixed with a 100 μL solution of TPPMS (5 mg/mL) in 0.1 M acetate buffer (pH 3.0) after filtration through a polycarbonate membrane with a pore diameter of 0.45 μm. After acidification to pH 3 with 0.1 N HCl, the reaction mixture was incubated at 37 °C for 1 h. The reaction mixture was analyzed by size-exclusion HPLC and TLC after filtration through a polycarbonate membrane with a pore diameter of 0.45 μm. Each sample was also analyzed by RP-HPLC after filtration through a 10 kDa cutoff ultrafiltration membrane. The fecal homogenates and urine samples obtained at 24 h postinjection of [[^{99m}Tc](HYNIC−NGA)(tricine)$_2$] were also reacted with TPPMS by similar procedures, and the radioactivity in the reaction mixture was analyzed.

RESULTS

In Vitro Studies. HYNIC−NGA conjugate (Figure 1) was prepared by reaction of the active esters of SHNH with ϵ-amine residues of the NGA. Three HYNIC groups were attached per molecule of NGA as determined by measuring the hydrazine groups. After purification by the centrifuged column procedure, [[^{99m}Tc](HYNIC−NGA)(tricine)$_2$] was obtained with radiochemical yields over 95% as determined by size-exclusion HPLC and TLC. The reaction of [^{99m}Tc]tricine$_2$ with unmodified NGA resulted in only 5.4% of the radioactivity associated with protein. Figure 2 shows size-exclusion radiochromatograms of [[^{99m}Tc](HYNIC−NGA)(tricine)$_2$] before and after incubation in freshly prepared murine plasma for 24 h. The radioactivity associated with NGA fractions was unchanged before (98.7%) and after 24 h incubation (97.6%). Similar results were obtained by TLC analyses.

In Vivo Studies. The biodistribution of radioactivity after intravenous administration of [[^{99m}Tc](HYNIC−NGA)(tricine)$_2$] is summarized in Table 1. At 10 min postinjection, more than 92% of the injected radioactivity was accumulated in the liver. The radioactivity was gradually eliminated from the liver by hepatobiliary excretion as the major excretion route. At 24 h postinjection, over 38% of the injected radioactivity was still retained in the liver. During the same postinjection period, 38 and 14% of the injected radioactivity was excreted in the feces and urine, respectively.

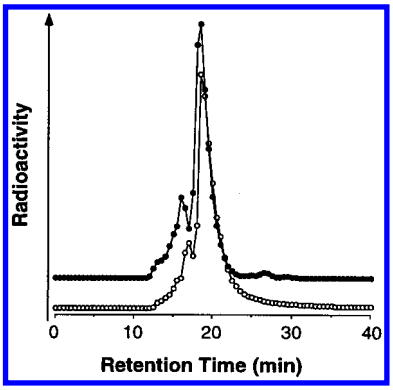

Figure 2. Size-exclusion radiochromatograms of [[^{99m}Tc]-(HYNIC−NGA)(tricine)$_2$] before (○) and after (●) incubation in freshly prepared murine plasma at 37 °C for 24 h.

Table 1. Biodistribution of Radioactivity after Intravenous Administration of [[^{99m}Tc](HYNIC−NGA)(tricine)$_2$] in Mice[a]

tissue	10 min[b]	30 min[b]	1 h[b]	3 h[b]	6 h[b]	24 h[b]
blood[c]	0.27	0.18	0.09	0.13	0.08	0.01
	(0.02)	(0.01)	(0.02)	(0.02)	(0.02)	(0.01)
liver	92.30	88.71	84.56	75.10	63.29	38.77
	(2.65)	(1.44)	(2.48)	(4.07)	(5.26)	(4.10)
intestine	0.36	4.34	7.61	14.54	20.88	2.23
	(0.09)	(0.62)	(0.91)	(0.97)	(2.14)	(0.52)
kidney	0.30	0.33	0.38	0.45	0.53	0.38
	(0.05)	(0.03)	(0.05)	(0.09)	(0.11)	(0.04)
spleen	0.08	0.08	0.08	0.09	0.06	0.04
	(0.04)	(0.01)	(0.01)	(0.03)	(0.01)	(0.03)
stomach	0.31	0.55	0.58	0.70	0.71	0.42
	(0.16)	(0.28)	(0.25)	(0.15)	(0.33)	(0.35)
feces						38.27
						(3.80)
urine						13.67
						(0.59)

[a] Expressed as % injected dose. Each value represents the mean (s.d.) for five animals at each interval. [b] Time after administration. [c] Expressed as percent dose per gram.

The Percoll density gradient centrifugation profiles of radioactivity in the liver at 1 and 24 h postinjection of [[^{99m}Tc](HYNIC−NGA)(tricine)$_2$] are illustrated in Figure 3. Each liver homogenate showed a major radioactivity peak at a density of ca. 1.10 g/mL, which correlated well with the β-galactosidase activity profiles.

The supernatants of the liver homogenates were obtained with radiochemical efficiencies of over 90%. After filtration of the liver supernatant at 1 and 24 h postinjection through the polycarbonate membrane, the radioactivity was recovered in the filtrates with 86.1 and 92.3% efficiencies, respectively. When analyzed by size-exclusion HPLC, while the liver supernatant at 1 h depicted a major radioactivity peak at a retention time close to that of [[^{99m}Tc](HYNIC−lysine)(tricine)$_2$] (Figure 4C), radioactivity was also detected in fractions over 10 kDa (Figure 4A). A significant increase in radioactive fractions over 10 kDa was observed with the liver supernatant at 24 h postinjection (Figure 4B). Under these conditions, the parental [[^{99m}Tc](HYNIC−NGA)-(tricine)$_2$] had a retention time of 18 min (Figure 4, panels A and B). On TLC analyses, the liver homogenates had radioactivity at the origin with a broad peak at R_f values of 0.5−0.65. The liver supernatant at 1 h postinjection was recovered in the filtrate with 76.3% efficiency after filtration through a 10 kDa cutoff ultrafiltration membrane, whereas the radioactivity recovered in the filtrate decreased to 54.3% after filtration of the liver supernatant at 24 h postinjection. RP-HPLC radiochromatograms

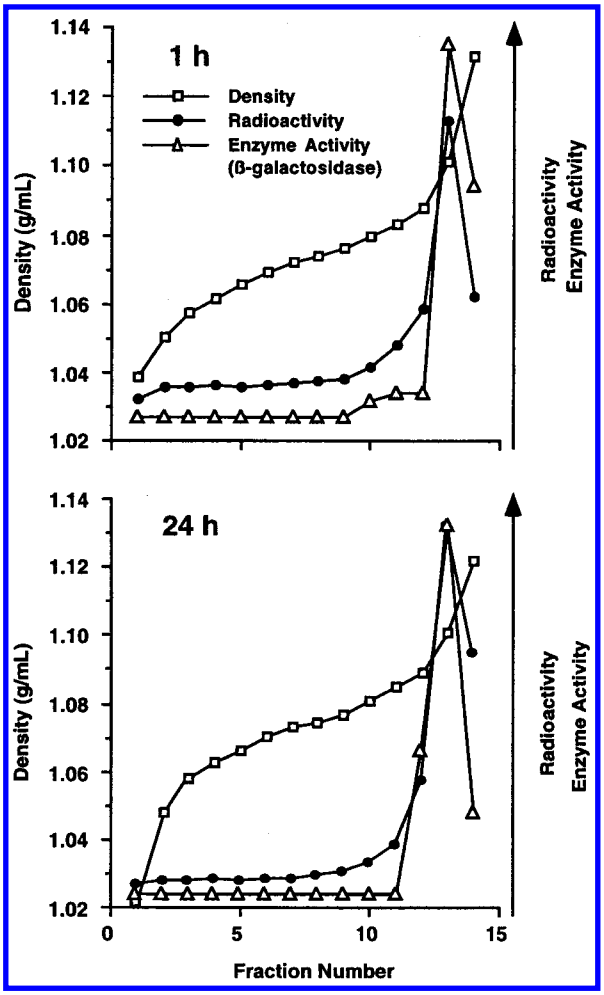

Figure 3. Percoll density gradient centrifugation profiles of liver homogenate at 1 and 24 h postinjection of [[^{99m}Tc](HYNIC−NGA)(tricine)$_2$]. In both preparations, a single radioactivity peak (●) that coincided with β-galactosidase activity (△) was detected at a density (□) of ca. 1.10 g/mL.

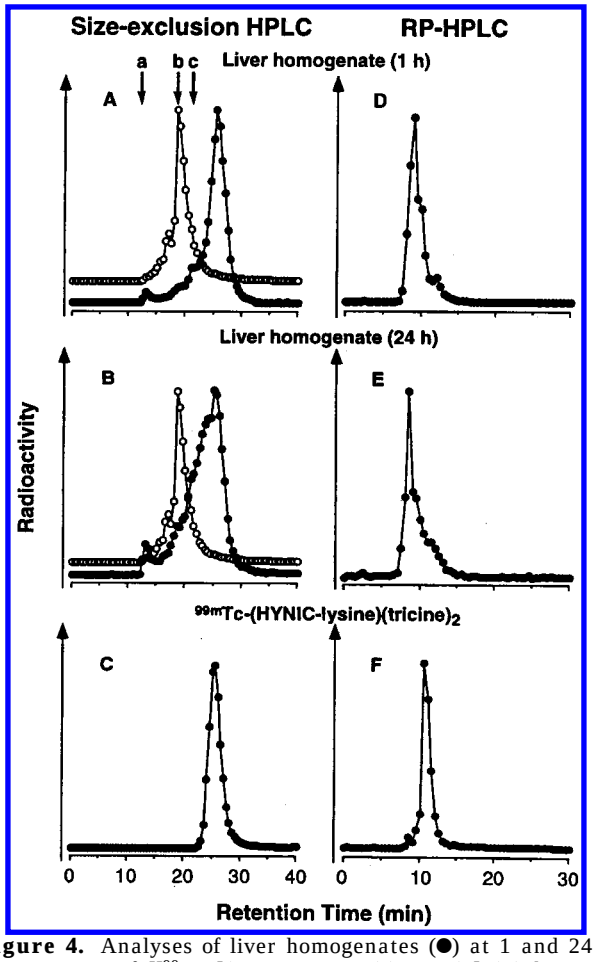

Figure 4. Analyses of liver homogenates (●) at 1 and 24 h postinjection of [[^{99m}Tc](HYNIC−NGA)(tricine)$_2$] (○) by size-exclusion HPLC (A and B) and RP-HPLC using solvent system 1 (D and E). Radiochromatograms of [[^{99m}Tc](HYNIC−lysine)-(tricine)$_2$] when analyzed by size-exclusion HPLC (C) and RP-HPLC (F). Under these conditions, thyroglobulin (a; 670 kDa), bovine serum albumin (b; 68 kDa) and cytochrome C (c; 13 kDa) had retention times of 13, 18, and 21 min, respectively, on size-exclusion HPLC.

of the liver supernatant at 1 and 24 h postinjection using the solvent system 1 are shown in Figure 4, panels D and E. Both supernatants showed similar radiochromatograms with a major radioactivity peak at a retention time of 8−9 min and a shoulder at a retention time of 11 min. Under these conditions, [[^{99m}Tc](HYNIC−lysine)-(tricine)$_2$] showed a radioactivity peak at a retention time of 11 min (Figure 4F). RP-HPLC analyses of the liver homogenates using solvent system 2 showed a radioactivity peak at a retention time of 4 min (Figure 6, panels A and B).

The radiochromatograms of the TPPMS-treated liver homogenates are illustrated in Figures 5 and 6. The radioactivity recovered in the filtrates was 91.1 and 88.6% after filtration of the TPPMS-homogenates obtained at 1 and 24 h postinjection through a polycarbonate membrane, respectively. On size-exclusion HPLC, a significant decrease in the radioactive fractions over 10 kDa was observed with TPPMS-treated liver homogenate at 24 h postinjection. The reaction product of [[^{99m}Tc]-(HYNIC−lysine)(tricine)$_2$] and TPPMS showed a single radioactivity peak at a retention time of 26 min on size-exclusion HPLC (Figure 5C). The radioactivity recovered in the filtrates increased to 89.2 and 91.1% for the TPPMS-treated liver homogenates obtained at 1 and 24 h postinjection after filtration through a 10 kDa cutoff ultrafiltration membrane. On RP-HPLC using solvent system 1, the TPPMS-treated liver homogenates showed a sharp radioactivity peak at a retention time of 17 min for both preparations, which was identical to that of the reaction product of [[^{99m}Tc](HYNIC−lysine)(tricine)$_2$] and TPPMS (Figure 5F). This was confirmed by co-chromatographic analyses (data not shown). Under these conditions, the reaction products of [^{99m}Tc]tricine$_2$ and TPPMS showed a radioactivity peak at a retention time of 13 min on RP-HPLC. Similar results were obtained on RP-HPLC analyses of the liver homogenates using solvent system 2, where both TPPMS-treated liver homogenates and [[^{99m}Tc](HYNIC−lysine)(tricine)$_2$] showed a single radioactivity peak at a retention time of 8.5 min, as shown in Figure 6. On TLC analyses, both TPPMS-treated liver homogenates and the reaction product of [[^{99m}Tc](HYNIC−lysine)(tricine)$_2$] and TPPMS showed a radioactivity peak at an R_f value of 0.7.

Figure 7 shows radiochromatograms of fecal and urine samples analyzed by size-exclusion HPLC and RP-HPLC using solvent system 1. Supernatants of feces were obtained with an efficiency of 54.6%. The recovered radioactivities in the filtrates after filtration though the polycarbonate membrane and the ultrafiltration membrane were 66.7 and 82.5% for feces and 96.9 and 98.3% for urine samples, respectively. Both fecal and urine samples showed a single radioactivity peak on size-exclusion HPLC at a retention time of 26 min (Figure 7, panels A and B). On RP-HPLC, a broad radioactivity

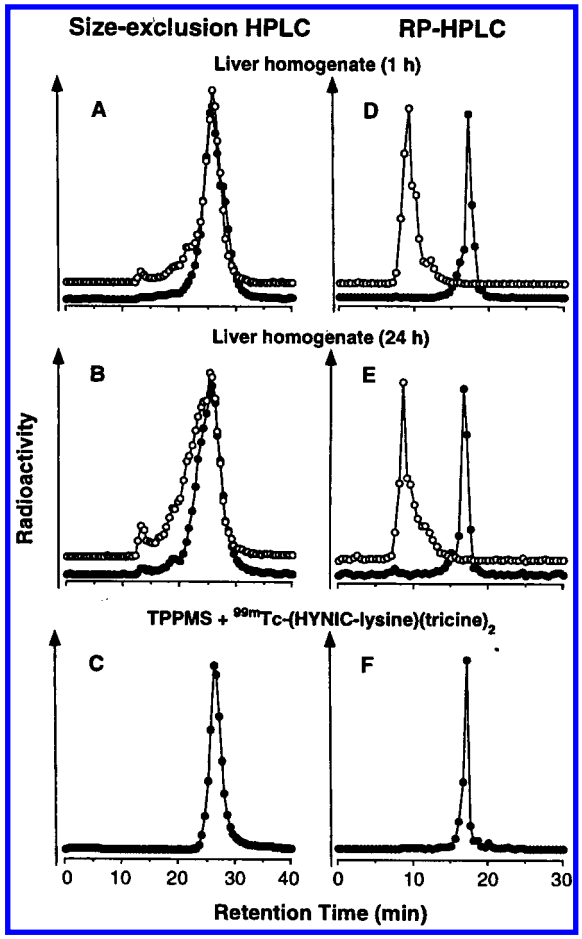

Figure 5. Radiochromatograms of liver homogenates at 1 and 24 h postinjection before (○) and after (●) TPPMS treatment by size-exclusion HPLC (A and B) and RP-HPLC using solvent system 1 (D and E). The reaction product of [[^{99m}Tc](HYNIC−lysine)(tricine)$_2$] with TPPMS was analyzed by size-exclusion HPLC (C) and RP-HPLC (F).

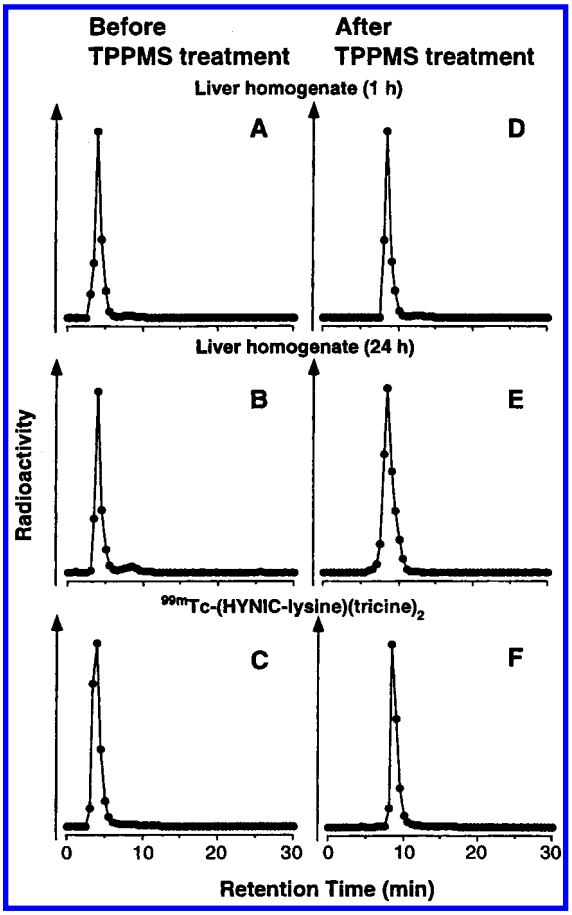

Figure 6. RP-HPLC radiochromatograms of liver homogenates at 1 and 24 h postinjection before and after treatment with TPPMS using solvent system 2. RP-HPLC radiochromatograms of [[^{99m}Tc](HYNIC−lysine)(tricine)$_2$] are also shown before and after treatment with TPPMS under similar conditions (C and F).

profile at a retention time of around 9 min was observed with both preparations using solvent system 1 (Figure 7, panels C and D). After TPPMS treatment, both feces and urine preparations showed migration of the radioactivity peaks to a retention time of 17 min, which was identical to that of the reaction product between [[^{99m}Tc](HYNIC−lysine)(tricine)$_2$] and TPPMS (Figure 7, panels E and F). Similar results were obtained by TLC analyses, where both preparations showed a radioactivity peak at an R_f value of 0.7 after TPPMS treatment.

DISCUSSION

Selective complexation of ^{99m}Tc to the HYNIC moiety was indicated by the exchange reaction of [^{99m}Tc]tricine$_2$ with HYNIC−NGA as shown by the small amounts of ^{99m}Tc attached to unmodified NGA. Unchanged size-exclusion HPLC radiochromatograms before and after incubation for 24 h in murine plasma reinforced the stable chemical bonding between ^{99m}Tc and HYNIC (Figure 2). In biodistribution studies, persistent localization of the radioactivity was observed in the murine liver in which catabolism of NGA occurs following the administration of [[^{99m}Tc](HYNIC−NGA)(tricine)$_2$] (Table 1). These findings using NGA as a model protein were in good agreement with those of previous studies using [^{99m}Tc]HYNIC-labeled proteins in experimental animals (*8*, *42*, *43*).

Radioactivity in the liver homogenates was copurified with lysosomes at 1 and 24 h postinjection of [[^{99m}Tc](HYNIC−NGA)(tricine)$_2$] (Figure 3), as observed in previous studies using ^{111}In-labeled NGAs with cDTPA or 1-(4-isothio,cyanatobenzyl)ethylenediaminetetraacetic acid (SCN−Bz-EDTA) as the BCAs (*24*, *26*, *31*, *44*, *45*). Previous studies also showed that both ^{111}In-labeled NGAs generated lysine-adducts ([^{111}In]DTPA-lysine and [^{111}In]SCN−Bz-EDTA-lysine) as the major final radiometabolites in murine hepatocytes and the slow elimination rates of the radiometabolites from the lysosomal compartment of hepatocytes are responsible for the persistent localization of the radioactivity in the liver. Since HYNIC was also conjugated to the ϵ-amine residues of NGA, lysine-adduct of HYNIC was prepared and radiolabeled with [^{99m}Tc]tricine$_2$ as a standard compound for subsequent analyses of the radioactivity retained in the liver and excreted in the urine and feces.

On size-exclusion HPLC analyses, the liver homogenates registered a radioactivity peak at a retention time representative of low molecular weight compounds such as [[^{99m}Tc](HYNIC−lysine)(tricine)$_2$] (Figure 4), as observed with ^{111}In-labeled NGAs. In contrast to ^{111}In-labeled NGAs, radiolabeled species were also registered in higher molecular weight fractions and the proportion of the fractions increased with postinjection interval. This was reflected in the decreased recovery of radioactivity in the filtrates of liver homogenates at 24 h postinjection using 10 kDa cutoff ultrafiltration membranes. Since generation of the final radiometabolites of ^{111}In-labeled NGAs was complete within 1 h postinjection (*24*, *30*), the time-dependent increase in high molecular weight frac-

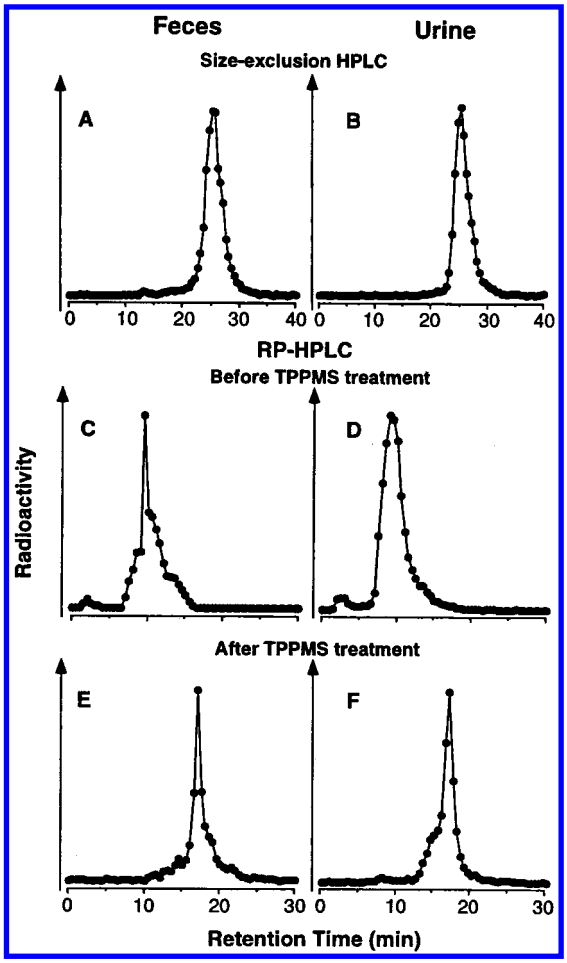

Figure 7. Analyses of feces and urine samples obtained at 24 h postinjection of [[^{99m}Tc](HYNIC−NGA)(tricine)$_2$] by size-exclusion HPLC (A and B) and RP-HPLC (C and D) using solvent system 1. After reacting with TPPMS, both preparations were analyzed by RP-HPLC (E and F).

tions suggested binding of radiometabolites derived from [[^{99m}Tc](HYNIC−NGA)(tricine)$_2$] with proteins present in the lysosomes, which would constitute a major reason for the long residence time of radioactivity in the liver.

To further understand the persistent localization of the radioactivity in the liver after administration of [[^{99m}Tc]-(HYNIC−NGA)(tricine)$_2$], radiolabeled species retained in the liver at the two postinjection intervals were analyzed. Both liver homogenates showed a broad radioactivity peaked at a retention time close to that of [[^{99m}Tc](HYNIC−lysine)(tricine)$_2$] (Figure 4), suggesting that multiple radiolabeled species derived from [[^{99m}Tc]-(HYNIC−lysine)(tricine)$_2$] would be present in the liver homogenates. Since [[^{99m}Tc](HYNIC−lysine)(tricine)$_2$] showed no change in RP-HPLC radiochromatograms after removing excess ligands (data not shown), the broad radioactivity of the liver homogenates suggested the formation of new mixed ligand ^{99m}Tc complexes. On the other hand, the reaction mixture of the liver homogenates with TPPMS showed RP-HPLC radiochromatograms similar to that of the reaction product of [[^{99m}Tc](HYNIC−lysine)(tricine)$_2$] and TPPMS (Figures 5 and 6). A recent study of [^{99m}Tc]HYNIC-labeled peptides showed that [[^{99m}Tc](HYNIC−peptide)(tricine)$_2$] reacts with TPPMS to provide a new ternary mixed ligand complex [[^{99m}Tc]-(HYNIC−peptide)(tricine)(TPPMS)], in which one tricine co-ligand was replaced with one TPPMS molecule (*32*). It has also been reported that [[^{99m}Tc](HYNIC−peptide)-(tricine)$_2$] gradually decomposed to hydrophilic ^{99m}Tc species in a dilute solution (*12*). Furthermore, the binding of [^{99m}Tc]HYNIC-labeled antibodies and DNA with serum proteins was observed (*11*, *46*). Thus, the findings in this study, together with those results of previous studies, suggested that [[^{99m}Tc](HYNIC−lysine)(tricine)$_2$] would be generated as the final radiometabolite after lysosomal proteolysis of [[^{99m}Tc](HYNIC−NGA)(tricine)$_2$] in the murine liver. However, one of the two tricine co-ligands of the metabolite would be replaced with amino acids to generate new mixed ligand ^{99m}Tc complexes of high protein binding ability or with amine residues of proteins present in the organelles, facilitated by a low pH environment in the absence of excess co-ligand.

The radiolabeled species excreted in the urine and feces were present as multiple low molecular weight compounds (Figure 7). However, since the TPPMS-treatment of urine samples and fecal extracts showed migration of the radioactivity with a retention time similar to that of [[^{99m}Tc](HYNIC−lysine)(tricine)(TPPMS)] on RP-HPLC, the radiolabeled species excreted from the body appeared to still retain the [[^{99m}Tc]HYNIC−tricine] bond in the absence of excess co-ligands. The multiple peaks in urine and feces determined by RP-HPLC also suggested the participation of amino acids in the mixed ligand [^{99m}Tc]-HYNIC complexes generated in the lysosomes of the liver.

In conclusion, the findings in this study implied that the bonding between ^{99m}Tc and HYNIC is extremely stable at low pH in the absence of excess co-ligands. The persistent localization of radioactivity in the liver after administration of [[^{99m}Tc](HYNIC−NGA)(tricine)$_2$] was attributed to the slow elimination rate of the final radiometabolite, [[^{99m}Tc](HYNIC−lysine)(tricine)$_2$] from the lysosomes, and subsequent replacement of one of the tricine co-ligands with amino acids to generate new ternary mixed ligand complexes of high protein binding ability or with amine residues of proteins in the lysosomes, presumably due to the low pH environment of the organelles and the absence of excess co-ligands. These findings also suggested that the development of appropriate co-ligands that form stable [^{99m}Tc]HYNIC−[co-ligand] mixed complexes at low pH in the absence of excess co-ligands is essential to reduce localization of radioactivity in nontarget tissues after administration of ^{99m}Tc-labeled proteins using HYNIC.

LITERATURE CITED

(1) Barrett, J. A., Damphousse, D. J., Heminway, S. J., Liu, S., Edwards, D. S., Looby, R. J., and Carroll, T. R. (1996) Biological evaluation of ^{99m}Tc-labeled cyclic glycoprotein IIb/IIIa receptor antagonists in the canine arteriovenous shunt and deep vein thrombosis models: effects of [^{99m}Tc]chelator-peptide conjugates. *Bioconjugate Chem. 7*, 203−208.

(2) Vallabhajosula, S., Moyer, B. R., James, J. L., McBride, B. J., Lipszyc, H., Lee, H., Bastidas, D., and Dean, R. T. (1996) Preclinical evaluation of technetium-99m-labeled somatostatin receptor-binding peptides. *J. Nucl. Med. 37*, 1016−1022.

(3) Verhaar, M. J., Keep, P. A., Hawkins, R. E., Robson, L., Casey, J. L., Pedley, B., Borden, J. A., Begent, R. H. J., and Chester, K. A. (1996) Technetium-99m radiolabeling using a phage-derived single-chain Fv with a C-terminal cysteine. *J. Nucl. Med. 37*, 868−872.

(4) Vanbilloen, H. P., Bormans, G. M., Deroo, M. J., and Verbruggen, A. M. (1995) Complexes of technetium-99m with tetrapeptides, a new class of Tc-99m-labelled agents. *Nucl. Med. Biol. 22*, 325−338.

(5) Pearson, D. A., Lister James, J., McBride, W. J., Wilson, D. M., Martel, L. J., Civitello, E. R., Taylor, J. E., Moyer, B. R., and Dean, R. T. (1996) Somatostatin receptor-binding peptides labeled with technetium-99m: chemistry and initial biological studies. *J. Med. Chem. 39*, 1361−1371.

(6) Bogdanov, A. J., Petherick, P., Marecos, E., and Weissleder, R. (1997) In vivo localization of diglycylcysteine-bearing synthetic peptides by nuclear imaging of oxotechnetate transchelation. *Nucl. Med. Biol. 24*, 739−742.

(7) Chang, F., Rusckowski, M., Qu, T., and Hnatowich, D. J. (1997) Early results in the irrational design of new bifunctional chelators. *Cancer 80*, 2347−2353.

(8) Abrams, M. J., Juweid, M., tenKate, C. I., Schwartz, D. A., Hauser, M. M., Gaul, F. E., Fuccello, A. J., Rubin, R. H., Strauss, H. W., and Fischman, A. J. (1990) Technetium-99m-human polyclonal IgG radiolabeled via the hydrazino nicotinamide derivative for imaging focal sites of infection in rats. *J. Nucl. Med. 31*, 2022−2028.

(9) Babich, J. W., Graham, W., Barrow, S. A., Dragotakes, S. C., Tompkins, R. G., Rubin, R. H., and Fischman, A. J. (1993) Technetium-99m-labeled chemotactic peptides: comparison with indium-111-labeled white blood cells for localizing acute bacterial infection in the rabbit. *J. Nucl. Med. 34*, 2176−2181.

(10) Verbeke, K., Hjelstuen, O., Debrock, E., Cleynhens, B., De Roo, M., and Verbruggen, A. (1995) Comparative evaluation of $^{99}Tc^{m}$-Hynic-HSA and $^{99}Tc^{m}$-MAG_3−HSA as possible blood pool agents. *Nucl. Med. Commun. 16*, 942−957.

(11) Hnatowich, D. J., Winnard, P., Jr., Virzi, F., Fogarasi, M., Sano, T., Smith, C. L., Cantor, C. R., and Rusckowski, M. (1995) Technetium-99m labeling of DNA oligonucleotides. *J. Nucl. Med. 36*, 2306−2314.

(12) Liu, S., Edwards, D. S., Looby, R. J., Harris, A. R., Poirier, M. J., Barrett, J. A., Heminway, S. J., and Carroll, T. R. (1996) Labeling a hydrazino nicotinamide-modified cyclic IIb/IIIa receptor antagonist with ^{99m}Tc using aminocarboxylates as coligands. *Bioconjugate Chem. 7*, 63−71.

(13) Ultee, M. E., Bridger, G. J., Abrams, M. J., Longley, C. B., Burton, C. A., Larsen, S. K., Henson, G. W., Padmanabhan, S., Gaul, F. E., and Schwartz, D. A. (1997) Tumor imaging with technetium-99m-labeled hydrazinonicotinamide-Fab′ conjugates. *J. Nucl. Med. 38*, 133−138.

(14) Larsen, S. K., Solomon, H. F., Caldwell, G., and Abrams, M. J. (1995) [^{99m}Tc]tricine: a useful precursor complex for the radiolabeling of hydrazinonicotinate protein conjugates. *Bioconjugate Chem. 6*, 635−638.

(15) Abrams, M. J., Larsen, S. K., Shaik, S. N., and Zubieta, J. (1991) Investigation of techenetium-organohydrazine coordination chemistry. The crystal and molecular structure of $[TcCl_2(C_8H_5N_4)(PPh_3)_2]\cdot 0.75C_7H_8$ and $[TcNCl_2(PPh_3)_2]\cdot 0.25CH_2Cl_2$. *Inorg. Chim. Acta 185*, 7−15.

(16) Abrams, M. J., Larsen, S. K., and Zubieta, J. (1991) Investigation of the technetium-hydrazido core. Synthesis and structural characterization of $[(n\text{-}C_4H_9)N][Tc_2(NNPh_2)_2(C_6Cl_4O_2)_4]\cdot CH_2Cl_2\cdot 2CH_3OH$, a Tc(V)/Tc(IV) catecholate complex with the hydrazido ligands adopting the unusual n1 bridging model. *Inorg. Chem. 30*, 2031−2035.

(17) Nicholson, T., Cook, J., Davison, A., Rose, D. J., Maresca, K. P., Zubieta, J. A., and Jones, A. J. (1996) The synthesis and characterization of $[MCl_3(N{=}NC_5H_4NH)(HN{=}NC_5H_4N)]$ from $[MO_4]^-$ (where M = Re, Tc) organodiazenido, organodiazene-chelate complexes. The X-ray structure of $[ReCl_3(N{=}NC_5H_4NH)(HN{=}NC_5H_4N)]$. *Inorg. Chim. Acta 252*, 421−426.

(18) Nicholson, T., Cook, J., Davison, A., Rose, D. J., Maresca, K. P., Zubieta, J. A., and Jones, A. J. (1996) The synthesis, characterization and X-ray crystal structure of the rhenium organodiazenido, organodiazene complex of $[ReCl_2(PPh_3)(N{=}NC_5H_4NH)(HN{=}NC_5H_4N)]$. *Inorg. Chim. Acta 252*, 427−430.

(19) Liu, S., Edwards, D. S., and Barrett, J. A. (1997) ^{99m}Tc Labeling of highly potent small peptides. *Bioconjugate Chem. 8*, 621−636.

(20) Callahan, R. J., Barrow, S. A., Abrams, M. J., Rubin, R. H., and Fischman, A. J. (1996) Biodistribution and dosimetry of technetium-99m-hydrazino nicotinamide IgG: comparison with indium-111-DTPA-IgG. *J. Nucl. Med. 37*, 843−846.

(21) Claessens, R. A., Boerman, O. C., Koenders, E. B., Oyen, W. J., van der Meer, J. W., and Corstens, F. H. (1996) Technetium-99m labelled hydrazinonicotinamide human non-specific polyclonal immunoglobulin G for detection of infectious foci: a comparison with two other technetium-labelled immunoglobulin preparations. *Eur. J. Nucl. Med. 23*, 414−421.

(22) Claessens, R. A., Koenders, E. B., Oyen, W. J. G., and Corstens, F. H. (1996) Retention of technetium-99m in infectious foci in rats after release from technetium-99m labelled human non-specific polyclonal immunoglobulin G: a dual-label study with hydrazinonicotinamide and iminothiolano immunoglobulin. *Eur. J. Nucl. Med. 23*, 1536−1539.

(23) Akizawa, H., Arano, Y., Uezono, T., Ono, M., Fujioka, Y., Uehara, T., Yokoyama, A., Akaji, K., Kiso, Y., and Saji, H. (1998) Renal metabolism of ^{111}In-DTPA-D-Phe^1-octreotide in vivo. *Bioconjugate Chem. 9*, 662−670.

(24) Arano, Y., Mukai, T., Uezono, T., Wakisaka, K., Motonari, H., Akizawa, H., Taoka, Y., and Yokoyama, A. (1994) A biological method to evaluate bifunctional chelating agents to label antibodies with metallic radionuclides. *J. Nucl. Med. 35*, 890−898.

(25) Bass, L. A., Lanahan, M. V., Duncan, J. R., Erion, J. L., Srinivasan, A., Schmidt, M. A., and Anderson, C. J. (1998) Identification of the soluble in vivo metabolites of indium-111-diethylenetriaminepentaacetic acid-D-Phe^1-octreotide. *Bioconjugate Chem. 9*, 192−200.

(26) Duncan, J. R., and Welch, M. J. (1993) Intracellular metabolism of indium-111-DTPA-labeled receptor targeted proteins. *J. Nucl. Med. 34*, 1728−1738.

(27) Franano, F. N., Edwards, W. B., Welch, M. J., and Duncan, J. R. (1994) Metabolism of receptor targeted In-111-DTPA-glycoproteins: identification of In-111-DTPA-epsilon-lysine as the primary metabolic and excretory product. *Nucl. Med. Biol. 21*, 1023−1034.

(28) Alberts, B., Bray, D., Lewis, J., Raff, M., Roberts, K., and Watson, J. D. (1983) Membrane transport of macromolecules and particles; exocytosis and endocytosis. *Molecular Biology of The Cell*, pp 302−317, Garland Publishing Inc. New York.

(29) Ashwell, G., and Harford, J. (1982) Carbohydrate-specific receptors of the liver. *Annu. Rev. Biochem. 51*, 531−554.

(30) Arano, Y., Mukai, T., Akizawa, H., Uezono, T., Motonari, H., Wakisaka, K., Kairiyama, C., and Yokoyama, A. (1995) Radiolabeled metabolites of protein play a critical role in radioactivity elimination from the liver. *Nucl. Med. Biol. 22*, 555−564.

(31) Rogers, B. E., Franano, F. N., Duncan, J. R., Edwards, W. B., Anderson, C. J., Connett, J. M., and Welch, M. J. (1995) Identification of metabolites of In-111-diethylenetriaminepentaacetic acid monoclonal antibodies and antibody fragments in vivo. *Cancer Res. 55*, S5714−S5720.

(32) Edwards, D. S., Liu, S., Barrett, J. A., Harris, A. R., Looby, R. J., Ziegler, M. C., Heminway, S. J., and Carroll, T. R. (1997) New and versatile ternary ligand system for technetium radiopharmaceuticals: water soluble phosphines and tricine as coligands in labeling a hydrazinonicotinamide-modified cyclic glycoprotein IIb/IIIa receptor antagonist with ^{99m}Tc. *Bioconjugate Chem. 8*, 146−54.

(33) Lee, Y. C., Stowell, C. P., and Krantz, M. J. (1976) 2-Imino-2-methoxyethyl 1-thioglycosides: new reagents for attaching sugars to proteins. *Biochemistry 15*, 3956−3963.

(34) Stowell, C. P., and Lee, Y. C. (1980) Preparation of some new neoglycoproteins by amidination of bovine serum albumin using 2-imino-2-methoxyethyl 1-thioglycosides. *Biochemistry 19*, 4899−4904.

(35) Dubois, M., Gilles, K. A., Hamilton, J. K., Rebers, P. A., and Smith, F. (1956) Colorimetric method for determination of sugars and related substances. *Anal. Chem. 28*, 350−356.

(36) King, T. P., Zhao, S. W., and Lam, T. (1986) Preparation of protein conjugates via intermolecular hydrazone linkage. *Biochemistry 25*, 5774−5779.

(37) Meares, C. F., McCall, M. J., Reardan, D. T., Goodwin, D. A., Diamanti, C. I., and McTigue, M. (1984) Conjugation of antibodies with bifunctional chelating agents: isothiocyanate and bromoacetamide reagents, methods of analysis, and subsequent addition of metal ions. *Anal. Biochem. 142*, 68−78.

(38) Imai, S., Morimoto, J., Tsubura, T., Esaki, K., Michalides, R., Holms, R. S., Deimling, O., and Higlgers, J. (1986) Genetic

marker patterns and endogenous mammary tumor virus genes in inbred mouse strains in Japan. *Exp. Anim. 35*, 263−276.

(39) Alquier, C., Guenin, P., Munari-Silem, Y., Audebet, C., and Rousset, B. (1985) Isolation of pig thyroid lysosomes. *Biochem. J. 232*, 529−537.

(40) Caimi, L., Marchesini, S., Aleo, M. F., Bresciani, R., Monti, E., Casella, A., Guidici, M. L., and Preti, A. (1989) Rapid preparation of a distinct lysosomal population from myelinating mouse brain using Percoll gradients. *J. Neurochem. 52*, 1722−1728.

(41) Distler, J., and Jourdian, G. W. (1978) B-Galactosidase from bovine testes. *Methods Enzymol. 50* (part C), 514−520.

(42) Fritzberg, A. R., Berninger, R. W., Hardley, S. W., and Wester, D. W. (1988) Approaches to radiolabeling of antibodies for diagnosis and therapy of cancer. *Pharm. Res. 5*, 325−334.

(43) Liu, S., Edwards, D. S., Looby, R. J., Poirier, M. J., Rajopadhye, M., Bourque, J. P., and Carroll, T. R. (1996) Labeling cyclic glycoprotein IIb/IIIa receptor antagonists with Tc-99m by the preformed chelate approach: Effects of chelators on properties of [Tc-99m]chelator-peptide conjugates. *Bioconjugate Chem. 7*, 196−202.

(44) Arano, Y., Mukai, T., Uezono, T., Motonari, H., Wakisaka, K., and Yokoyama, A. (1994) Biological comparison of DTPA and SCN−Bz-EDTA as a chelating agent for indium labeling of antibodies. *J. Laballed Compd. Radiopharm. 35*, 381−383.

(45) Mukai, T., Arano, Y., Nishida, K., Sasaki, H., Saji, H., and Nakamura, J. (1999) Pharmacokinetic estimation of ^{111}In-DTPA-labeling for assessment of sites of protein catabolism in vivo. *J. Pharm. Pharmacol. 51*, 15−20.

(46) Hnatowich, D. J., Mardirossian, G., Rusckowski, M., Fogarasi, M., Virzi, F., and P. Winnard, J. (1993) Directly and indirectly technetium-99m-labeled antibodies-a comparison of in vitro and animal in vivo properties. *J. Nucl. Med. 34*, 109−119.

BC980105F